THREE SECTIONS CIRCULAR WAVEGUIDE APERTURE ANTENNA WITH CONICAL BEAM

S. Qi, W. Wu, and D. Fang

Ministerial Key Laboratory of JGMT
Nanjing University of Science and Technology, Nanjing 210094, China

Abstract—A three sections circular waveguide aperture antenna with conical beam is presented. By using two waveguide steps, the aperture distribution of the antenna can be controlled to realize the requirements on the radiation pattern with conical beam including the flare angle, gain and the side lobe level. Through optimized design, the impedance bandwidth of $550\,\text{MHz}$ with $-10\,\text{dB}$ return loss, the gain of $8.1\,\text{dB}$ and a flare angle of 50 degrees have been achieved at the central frequency $35\,\text{GHz}$. Good agreement has been observed between simulated results and measured ones. The proposed antenna is easy to be fabricated and suitable for many applications.

1. INTRODUCTION

Antennas with a conical beam have been required for communications between base stations and moving vehicles. The demand of conical beam antennas is also increasing in wireless network systems, consisting of numerous indoor base station antennas, because they can cover a large service area and provide a stable signal quality [1]. Recently, printed antennas have been employed in obtaining conical beam. TM_{01} mode of the circular patch antennas have been reported to produce a conical beam pattern [2]. However, the design has difficulty with side lobe level control when the size of the patch increases to obtain high gain and large flare angle. In [3, 4] multiple antenna elements which are arranged in a circular topology have been proposed to generate an omni-directional radiation pattern. Some of them are either poor azimuth symmetry or with a complicated feeding network. A GA-based design of multi-ring arrays with omni-directional conical beam pattern has been reported [5]. However it also needs complicated feeding network.

In this paper, a three sections circular waveguide aperture antenna with a conical beam is presented. Two circular waveguide steps are introduced to control the aperture distribution of the antenna for the purpose of realizing the required beam and the impedance matching. A coaxial line is used to feed this three sections circular waveguide aperture antenna from the bottom. The formally exact mode matching method [6–16] is known to be one of the most efficient and accurate method for analyzing such regular structures. It is therefore employed in predicting the return loss and radiation pattern of the proposed three sections circular waveguide aperture antenna. Numerical results for the scattering parameters and radiation patterns agree well with measured ones. The designed antenna exhibits good return loss, side lobe level, flare angle, and gain performance in the $-10\,$dB impedance bandwidth of 550 MHz at the central frequency of 35 GHz.

2. DESCRIPTION OF THE ANTENNA CONFIGURATION

Conical beam can be easily obtained by exciting TM_{0m} modes in an open ended circular waveguide. Figure 1 shows the geometry of the three sections circular waveguide aperture antenna fed by a coaxial line. The antenna can be divided into five parts: two coaxial lines, two circular waveguides and one open ended circular waveguide. As indicated in Figure 1, the inner and outer radii of the coaxial feed line are a and b, respectively. The radii of the i-th circular waveguide is, respectively R_i for $i = 1, 2, 3$. The length of the i-th circular waveguide is, respectively L_i for $i = 1, 2, 3$. The length of the inner conductor of
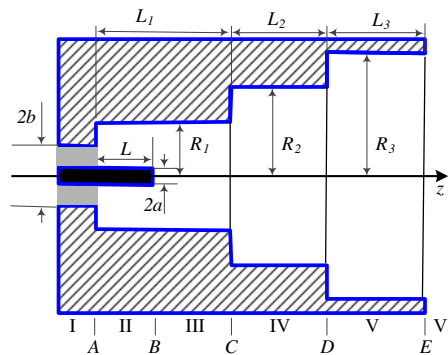

Figure 1. The geometry of the three sections circular waveguide aperture antenna fed by a coaxial line.

the coaxial line embed in the first circular waveguide is L.

The radiation pattern of the TM_{0m} mode for an open ended circular waveguide is [17]

$$E_\theta = B \frac{k_0 e^{-jk_0 r_{far}}}{2r_{far}} \frac{k_0 \sin\theta J_1(x_m) J_0(k_0 \sin\theta R)}{\sqrt{\pi} J_1(x_m)[(x_m/R)^2 - (k_0 \sin\theta)^2]} \qquad (1)$$

where θ is the flare angle in elevation plane, J_0 and J_1 are the Bessel functions of the first kind with zero order and first order, x_m is the m-th zero point of J_0, R is the radius of the open ended circular waveguide, k_0 is the wavenumber in free space, and r_{far} is the distance between antenna and observation point of far field. The flare angle θ is determined by R and the main TM mode being used. Figures 2 and 3 show the magnitude and phase of the radiation pattern corresponding to the TM_{0m} ($m = 1, 2, 3, 4$) mode of the open ended circular waveguide with radius equal to $15\,mm$, respectively. It can be seen that beam
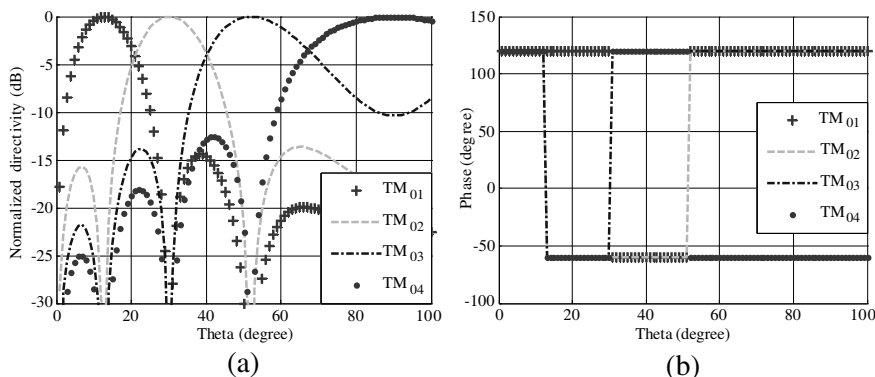

Figure 2. The radiation pattern corresponding to the TM_{0m} ($m = 1, 2, 3, 4$) mode of the open ended circular waveguide with radius of $15\,mm$. (a) Magnitude, and (b) phase.
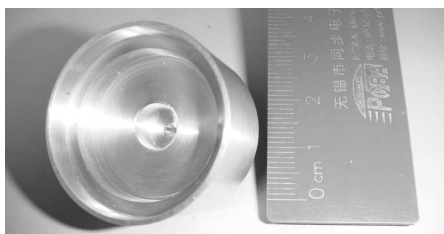

Figure 3. Photograph of the fabricated three sections circular waveguide aperture antenna fed by a coaxial line.

direction moves to 90 degrees when m increases from 1 to 4 and phase of the radiation pattern alternates between 120 degrees and -60 degrees. Due to the fact, the magnitude and phase of every mode can be controlled to synthesize our desired radiation pattern by introducing several waveguide steps. In this paper, TM_{03} mode has been selected as the main TM mode on the aperture of the antenna while TM_{01} and TM_{02} modes mainly contribute to the side lobe. Therefore, R_3 can be determined using (1) due to the desired beam direction and the main TM mode being used while R_1 can be determined by requirement of only TM_{01} mode propagation. In order to obtain good side lobe level performance, R_2, L_2 and L_3 of waveguide steps are tuned to suppress the proportion of TM_{01} and TM_{02} modes on the aperture of the antenna. It should be noted that all other higher TM modes are cutoff modes. By properly adjusting L and L_1, good impedance matching for the proposed antenna can be realized.

3. MODE-MATCHING FORMULATION

Due to the fact that multiple parameters of the antenna need to be optimized, the efficient and accurate mode matching method [6–16] is employed as the modeling tool. As shown in Figure 1, both the structure and the incident TEM mode in the coaxial feed line are axis-symmetric ($\partial/\partial\phi = 0$), only the dominant TEM mode and TM_{0m} modes in these waveguides can be excited. Based on this property, we can derive the field expressions for all the sub-regions in Figure 1. There are five waveguide junctions in this antenna: the coaxial waveguide to coaxial waveguide, the coaxial waveguide to circular waveguide, the circular waveguide to circular waveguide and circular waveguide to free space. Referring to Figure 1, in regions I, II, III, IV and V, the transverse electromagnetic fields with respect to the z axis can be represented by

$$
\begin{cases}
\vec{E}_t^{\,i}(\rho) = \sum\limits_{m=1}^{M_i} \left(A_{i,0m}^+ e^{-\Gamma_{i,0m}z} + A_{i,0m}^- e^{\Gamma_{i,0m}z} \right) \vec{e}_{i,0m}(\rho) \\
\vec{H}_t^{\,i}(\rho) = \sum\limits_{m=1}^{M_i} \left(A_{i,0m}^+ e^{-\Gamma_{i,0m}z} - A_{i,0m}^- e^{\Gamma_{i,0m}z} \right) Y_{i,0m}\, \vec{z} \times \vec{e}_{i,0m}(\rho)
\end{cases}
\tag{2}
$$

where $A_{i,0m}^{\pm}$, $\Gamma_{i,0m}$, $Y_{i,0m}$, and $\vec{e}_{i,0m}(\rho)$ are the incident and reflected modal amplitude, the propagation constant, model admittance, and normalized transverse modal electric field of the TM_{0m} mode in the i-th waveguides (i = I, II, III, IV, V), respectively. The expression of $\vec{e}_{i,0m}(\rho)$ for coaxial waveguide and circular waveguide is available in [7].

Use of proper inner products and application of the boundary conditions that the tangential electromagnetic field components must be continuous across the junctions will lead to the electric and magnetic field matching equations [8]

$$
\begin{cases}
M_j(A_{j,1}^+ + A_{j,1}^-) = A_{j,2}^+ + A_{j,2}^- \\
Y_{j,1}(A_{j,1}^+ - A_{j,1}^-) = M_j^T Y_{j,2}(A_{j,2}^+ - A_{j,2}^-)
\end{cases}
\tag{3}
$$

where the superscript T represents the transpose operation, and M_j, $A_j^\pm$ and Y_j are the model mutual matrix, the incident and reflected modal amplitude column vector at each side of the j-th junction ($j = A, B, C, D$), model admittance diagonal matrix at each side of the j-th junction.

Therefore, S-parameters of the j-th junction can be easily obtained by

$$
\begin{cases}
S_{j,11} = (M_j^T Y_{j,2} M + Y_{j,1})^{-1}(Y_{j,1} - M_j^T Y_{j,2} M_j) \\
S_{j,21} = M_j(S_{j,11} + I) \\
S_{j,12} = Y_{j,1} S_{j,21}^T Y_{j,2} \\
S_{j,22} = M_j S_{j,12} - I
\end{cases}
\tag{4}
$$

The mode matching matrices at junctions E are available in [9]. After cascading the S-parameters of all junctions, we can obtain the modal expansion coefficients at the aperture and the reflection coefficient at the input port of the feed line. Once the expansion coefficients are known, the electric and magnetic field expressions can be obtained at the circular waveguide aperture, from which the overall radiation pattern can be finally obtained by superposing radiation pattern of each TM_{0m}.

By changing L, L_i, and R_i, the desired radiation pattern and return loss can be synthesized. However, it is very difficult to determine the optimal value of seven variations. Pareto genetic algorithm for multi-objective has been employed to synthesis the desired antenna radiation pattern and return loss. The individual of population is constructed as

$$
Q = [\; R_1 \quad R_2 \quad R_3 \quad L \quad L_1 \quad L_2 \quad L_3 \;],
\tag{5}
$$

which is the vector of variables to be optimized. The fitness function is assigned as

$$
\sum_{\theta=0}^{\pi/2} \left(20 \log \frac{E_{actual}(\theta, Q)}{E_{desired}(\theta)} \right)^2,
\tag{6}
$$

for radiation pattern and

$$
\sum_f (S_{actual}(Q, f) - S_{desired}(f))^2,
\tag{7}
$$

for reflection coefficient. $E_{actual}(\theta, Q)$ and $S_{actual}(Q, f)$ are the antenna radiation pattern and return loss respectively from our method. $E_{desired}(\theta)$ and $S_{desired}(f)$ are the objective radiation pattern and return loss as shown in Figures 4 and 5 respectively. The final optimal antenna parameters are given as follows: $a = 0.3\,\mathrm{mm}$, $b = 1\,\mathrm{mm}$, $R_1 = 4\,\mathrm{mm}$, $R_2 = 12.6\,\mathrm{mm}$, $R_3 = 15\,\mathrm{mm}$, $L = 2\,\mathrm{mm}$, $L_1 = 6.3\,\mathrm{mm}$, $L_2 = 4.6\,\mathrm{mm}$, $L_3 = 4.6\,\mathrm{mm}$.

4. SIMULATED AND MEASURED RESULTS

A three sections circular waveguide aperture antenna has been designed, fabricated and tested. The photograph of the fabricated antenna is shown in Figure 3. The return loss of the antenna is measured by a network analyzer Agilent E8722ES and radiation pattern is measured in an anechoic chamber. Figure 4 shows the simulated and measured return loss results of the fabricated antenna. The measured impedance bandwidth with $-10\,\mathrm{dB}$ return loss of the three sections circular waveguide aperture antenna is $550\,\mathrm{MHz}$ at $35\,\mathrm{GHz}$. Figure 5 provides the comparison between simulated radiation pattern and measured ones. Good agreement is observed. The measured flare angle and gain of the radiation pattern at $35\,\mathrm{GHz}$ is 50 degrees and $8.1\,\mathrm{dB}$ respectively. Simulated ripple of the radiation pattern in azimuth plan is $0.04\,\mathrm{dB}$. The discrepancies between simulated and measured results are owing to tolerance of manufacture and test instrument.
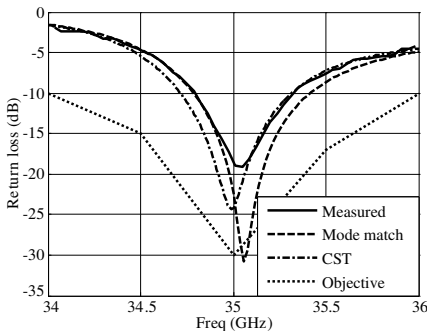

Figure 4. Simulated and measured return loss results of the coaxial-fed three sections circular waveguide aperture antenna.
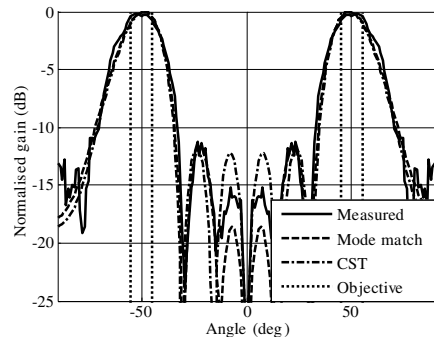

Figure 5. Simulated and measured radiation pattern results of the coaxial-fed three sections circular waveguide aperture antenna.

5. CONCLUSION

In this paper, a three sections circular waveguide aperture antenna with a conical beam has been designed, fabricated and tested. Two waveguide steps are introduced to optimize the return loss and radiation pattern of the three sections circular waveguide aperture antenna. Experimental results demonstrate that it can achieve a flare angle of 50 degrees, 8.1 dB gain and −11.3 dB side lobe levels. Measured results are in good agreement with simulated ones. The number of steps can be increased to satisfy more critical requirements. The proposed three sections circular waveguide aperture antenna in this paper is an effective structure to realize a conical beam.

REFERENCES

1. Wu, B. Q. and K.-M. Luk, "A wideband, low-profile, conical-beam antenna with horizontal polarization for indoor wireless communications," *IEEE Antennas Wirel. Propag. Lett.*, Vol. 8, 340–343, Jul. 2009.

2. Guo, Y.-X., M. W. Chia, Z. N. Chen, and K.-M. Luk, "Wide-band L-probe fed circular patch antenna for conical-pattern radiation," *IEEE Trans. Antennas Propag.*, Vol. 52, No. 4, 1115–1116, Apr. 2004.

3. Mcewan, N. J., R. A. Abd-alhameed, E. M. Ibrahim, P. S. Excell, and J. G. Gardiner, "A new design of horizontally polarized and dual-polarized uniplanar conical beam antennas for hiperlan," *IEEE Trans. Antennas Propag.*, Vol. 51, No. 2, 229–237, Feb. 2003.

4. Chen, K.-C., Y. Qian, C.-K. C. Tzuang, and T. Itoh, "A periodic microstrip radial antenna array with a conical beam," *IEEE Trans. Antennas Propag.*, Vol. 51, No. 4, 756–765, Apr. 2003.

5. Son, S.-H., S.-I. Jeon, C.-J. Kim, and W. Hwang, "GA-based design of multi-ring arrays with omnidirectional conical beam pattern," *IEEE Trans. Antennas Propag.*, Vol. 58, No. 5, 1527–1535, May 2010.

6. Safavi-naini, R. and R. H. Macphie, "On solving waveguide junction scattering problems by the conservation of complex power technique," *IEEE Trans. Microw. Theory Tech.*, Vol. 29, No. 4, 337–343, Apr. 1981.

7. Macphie, R. H., M. Opie, and C. R. Ries, "Input impedance of a coaxial line probe feeding a circular waveguide in the TM_{01}

mode," *IEEE Trans. Microw. Theory Tech.*, Vol. 38, No. 3, 334–337, Mar. 1990.

8. Shen, Z. and R. H. Macphie, "An improved modal expansion method for two cascaded junctions and its application to waveguide filters," *IEEE Trans. Microw. Theory Tech.*, Vol. 43, No. 12, 2719–2722, Dec. 1995.

9. Shen, Z.-X. and R. H. Macphie, "A simple method for calculating the reflection coefficient of open-ended waveguides," *IEEE Trans. Microw. Theory Tech.*, Vol. 45, No. 4, 546–548, Apr. 1997.

10. Jiang, Z., Z. Shen, and X. Shan, "Mode-matching analysis of waveguide j-junction loaded with an *h*-plane dielectric slab," *Journal of Electromagnetic Waves and Applications*, Vol. 16, No. 11, 1613–1614, 2002.

11. Park, J. K., "Scattering analysis from a gap in the inner conductor of a coaxial line," *Journal of Electromagnetic Waves and Applications*, Vol. 17, No. 1, 121–129, 2003.

12. Du, K., V. V. Varadan, and V. K. Varadan, "Estimation of reflection coefficients for an open-ended coaxial waveguide radiating into a chiral half-space," *Journal of Electromagnetic Waves and Applications*, Vol. 15, No. 5, 643–663, 2001.

13. Anastassiu, H. T., J. L. Volakis, and D. C. Ross, "The mode matching technique for electromagnetic scattering by cylindrical waveguides with canonical terminations," *Journal of Electromagnetic Waves and Applications*, Vol. 9, Nos. 11–12, 1363–1391, 1995.

14. Morgan, M. A. and F. K. Schwering, "Mode expansion solution for scattering by a material filled rectangular groove," *Journal of Electromagnetic Waves and Applications*, Vol. 12, No. 4, 467–468, 1998.

15. Li, L. W., L. Zhou, M. S. Leong, T. S. Yeo, and P. S. Kooi, "An open-ended circular waveguide with an infinite conducting flange covered by a dielectric hemi-spherical radome shell: Full-wave analysis and green dyadics," *Journal of Electromagnetic Waves and Applications*, Vol. 13, No. 4, 561–563, 1999.

16. Gentili, G. G., R. Nesti, and G. Pelosi, "Efficient analysis of a complete feeding system in corrugated circular waveguide," *Journal of Electromagnetic Waves and Applications*, Vol. 13, No. 12, 1631–1648, 1999.

17. Silver, S., *Microwave Antenna Theory and Design*, 336–341, McGraw-Hill, New York, 1949.